Accurate BER Approximation for OSTBCs With Estimated CSI in Correlated Rayleigh Fading

Lennert Jacobs and Marc Moeneclaey
Ghent University, TELIN Department, DIGCOM Group
Sint-Pietersnieuwstraat 41, B-9000 Gent, Belgium
{Lennert.Jacobs,Marc.Moeneclaey}@telin.ugent.be

***Abstract*—In this contribution, we present a novel closed-form bit error rate (BER) approximation for orthogonal space-time block codes employing rectangular quadrature amplitude modulation. The multiple-input multiple-output channel is assumed to be affected by arbitrarily spatially correlated Rayleigh fading. We consider a mismatched maximum-likelihood receiver that obtains the channel state information through pilot-based linear minimum mean-square error channel estimation. The presented BER approximation is shown to yield very accurate results over a wide range of signal-to-noise ratios.**

I. Introduction

By employing proper space-time coding, multiple-input multiple-output (MIMO) systems can take advantage of spatial diversity. Orthogonal space-time block coding [1], [2] is a particularly interesting transmit diversity technique, since it achieves full spatial diversity and leads to a remarkably simple symbol-by-symbol decoding algorithm, based on linear processing at the receiver. Owing to the beneficial properties of orthogonal space-time block codes (OSTBCs), their error performance has been studied extensively in the past. Exact bit error rate (BER) expressions for pulse amplitude modulation (PAM), quadrature amplitude modulation (QAM), and phase-shift keying (PSK) constellations can be found in [3] and [4] for correlated Rayleigh fading channels with perfect channel state information (PCSI). The exact symbol error probability (SEP) of coherent PSK and QAM over spatially correlated MIMO Nakagami-m fading channels was derived in [5]. Exact closed-form SEP expressions of arbitrary rectangular QAM for single- and multichannel diversity reception over independent but not-necessarily identically distributed Nakagami-m fading channels were presented in [6].

In many practical wireless applications, imperfect channel estimation by the receiver degrades the system performance, such that PCSI can no longer be assumed. Under the assumption of pilot-based linear minimum mean-square error (LMMSE) channel estimation, a closed-form BER expression was presented in [7] for PAM and square QAM constellations operating over independent and identically distributed (i.i.d.) Rayleigh fading channels. For square OSTBCs, the latter expression is shown to be exact. In case of spatially correlated MIMO channels, we provided BER approximations in [8] and [9] for Rayleigh and arbitrary fading distributions, respectively. The result from [8] is obtained by approximating the covariance matrix of the channel estimation error for high signal-to-noise ratio (SNR) and is asymptotically exact, yet restricted to square OSTBCs only. The approach from [9] is valid for square and non-square OSTBCs, but the resulting BER expression is generally not asymptotically exact.

In contrast with the high-SNR BER approximations from [8] and [9], which have limited accuracy for low and medium SNR, we derive in this contribution a novel generalized closed-form BER approximation that yields very accurate results from low to high SNR for square and non-square OSTBCs using rectangular QAM on arbitrarily spatially correlated Rayleigh MIMO channels. For any SNR, the presented approximation allows to accurately examine the impact of imperfect channel estimation and fading correlation on the BER. The analytical BER results for i.i.d. MIMO channels and square QAM in [7] can be considered as special cases of the generalized BER approximation. Moreover, the latter approximation converges to the asymptotically exact BER result from [8] for high SNR in case of square OSTBCs and square QAM constellations.

We denote by $\mathrm{vec}(\mathbf{X})$ the vector that is obtained by stacking the columns of the matrix $\mathbf{X}$, and by $\mathbf{A} \otimes \mathbf{B}$ the Kronecker product of the matrices $\mathbf{A}$ and $\mathbf{B}$. The norm of a vector $\mathbf{a}$ is denoted by $\|\mathbf{a}\|$.

II. Signal model

Let us consider a wireless MIMO communication system using L_t transmit and L_r receive antennas. Assuming OSTBCs from complex orthogonal designs [2], [10], each OSTBC transforms N_s information symbols $s_i = s_{i,\mathrm{R}} + js_{i,\mathrm{I}}$, $1 \leq i \leq N_\mathrm{s}$, with $s_{i,\mathrm{R}}$ and $s_{i,\mathrm{I}}$ denoting the real and imaginary parts of s_i, respectively, into an $L_\mathrm{t} \times K_\mathrm{c}$ coded symbol matrix $\mathbf{C}$, the entries of which are linear combinations of s_i and their complex conjugate s_i^*

$$\mathbf{C} = \sum_{i=1}^{N_\mathrm{s}} \left(\mathbf{C}_i \, s_i + \mathbf{C}_i^{'} \, s_i^* \right), \tag{1}$$

where the $L_\mathrm{t} \times K_\mathrm{c}$ matrices $\mathbf{C}_i$ and $\mathbf{C}_i^{'}$ consist of the coefficients of s_i and s_i^*, respectively. We assume that $\mathbf{C}$ is scaled in such way that it satisfies the following orthogonality condition

$$\mathbf{C}\mathbf{C}^H = \lambda \|\mathbf{s}\|^2 \mathbf{I}_{L_\mathrm{t}}, \tag{2}$$

where $\lambda \triangleq K_\mathrm{c}/N_\mathrm{s}$, $\mathbf{s} = [s_1, s_2, \ldots, s_{N_\mathrm{s}}]^T$ is the information symbol vector, and $\mathbf{I}_{L_\mathrm{t}}$ denotes the $L_\mathrm{t} \times L_\mathrm{t}$ identity matrix. From the orthogonality condition (2), it follows that

$$\frac{1}{L_\mathrm{t} K_\mathrm{c}} \mathbb{E}[\|\mathbf{C}\|^2] = 1. \tag{3}$$

978-1-4673-5939-9/13/$31.00 ©2013 IEEE

For square OSTBCs, i.e., when $K_{\mathrm{c}} = L_{\mathrm{t}}$, the orthogonality criterion (2) can be extended to

$$\mathbf{C}^H\mathbf{C} = \mathbf{C}\mathbf{C}^H = \lambda\|\mathbf{s}\|^2\mathbf{I}_{L_{\mathrm{t}}}. \tag{4}$$

The transmitter is assumed to use data frames associating K_{p} time slots to pilot symbols and K time slots to coded data symbols, with K being a multiple of K_{c}. In this way, each data frame comprises K/K_{c} coded data matrices $\mathbf{C}(k)$, $1 \leq k \leq K/K_{\mathrm{c}}$. Note that we use orthogonal pilot sequences to estimate the channel state information, i.e., the $L_{\mathrm{t}} \times K_{\mathrm{p}}$ pilot matrix $\mathbf{C}_{\mathrm{p}}$ has orthogonal rows such that

$$\mathbf{C}_{\mathrm{p}}\mathbf{C}_{\mathrm{p}}^H = K_{\mathrm{p}}\mathbf{I}_{L_{\mathrm{t}}}. \tag{5}$$

The $L \triangleq L_{\mathrm{t}}L_{\mathrm{r}}$ coefficients of a MIMO channel are usually represented by an $L_{\mathrm{r}} \times L_{\mathrm{t}}$ complex-valued random matrix $\mathbf{H}$. However, in order to allow a simple characterization of the correlation between the channel coefficients, we stack the elements of the channel matrix $\mathbf{H}$ into the column vector $\mathbf{h} \triangleq \mathrm{vec}(\mathbf{H})$, the elements of which are assumed to be arbitrarily correlated zero-mean (ZM) circularly symmetric complex Gaussian (CSCG) random variables (RVs) with a positive definite covariance matrix $\boldsymbol{\mathcal{R}} \triangleq \mathbb{E}[\mathbf{h}\mathbf{h}^H]$. Adopting the MIMO vector model from [11], the received signals corresponding to the OSTBC matrices $\mathbf{C}(k)$ and the pilot matrix $\mathbf{C}_{\mathrm{p}}$, respectively, are given by

$$\mathbf{r}(k) = \sqrt{E_{\mathrm{s}}}\,\mathbf{B}(k)\,\mathbf{h} + \mathbf{w}(k), \tag{6a}$$

$$\mathbf{r}_{\mathrm{p}} = \sqrt{E_{\mathrm{p}}}\,\mathbf{B}_{\mathrm{p}}\,\mathbf{h} + \mathbf{w}_{\mathrm{p}}, \tag{6b}$$

where the channel $\mathbf{h}$ is assumed to remain constant during the length of one frame of $K+K_{\mathrm{p}}$ symbols, and $\mathbf{B}(k) \triangleq \mathbf{C}(k)^T \otimes \mathbf{I}_{L_{\mathrm{r}}}$ and $\mathbf{B}_{\mathrm{p}} \triangleq \mathbf{C}_{\mathrm{p}}^T \otimes \mathbf{I}_{L_{\mathrm{r}}}$. In the remainder of the paper, we drop the block index k in (6a) for simplicity of notation. From (2) and (5), it is readily verified that $\mathbf{B}^H\mathbf{B} = \lambda\|\mathbf{s}\|^2\mathbf{I}_L$ and $\mathbf{B}_{\mathrm{p}}^H\mathbf{B}_{\mathrm{p}} = K_{\mathrm{p}}\mathbf{I}_L$, respectively. The additive channel noise vectors $\mathbf{w}$ and $\mathbf{w}_{\mathrm{p}}$ affecting the transmission of the data and pilot symbols, respectively, consist of i.i.d. ZM CSCG RVs with variance N_0. Using a normalized symbol constellation, i.e.,

$$\mathbb{E}\left[\|s_i\|^2\right] = 1, \tag{7}$$

it follows from (3) and (5) that E_{s} and E_{p} in (6a) and (6b) denote the average data and pilot symbol energy, respectively.

III. Pilot-based channel estimation

We assume LMMSE channel estimation, which yields [11]

$$\hat{\mathbf{h}} = \frac{\sqrt{E_{\mathrm{p}}}}{N_0}\left(\mathbf{I}_L + \frac{K_{\mathrm{p}}E_{\mathrm{p}}}{N_0}\boldsymbol{\mathcal{R}}\right)^{-1}\boldsymbol{\mathcal{R}}\,\mathbf{B}_{\mathrm{p}}^H\,\mathbf{r}_{\mathrm{p}}. \tag{8}$$

With $\boldsymbol{\varepsilon} \triangleq \mathbf{h}-\hat{\mathbf{h}}$ being the channel estimation error, it is readily verified that $\boldsymbol{\varepsilon}$ and $\hat{\mathbf{h}}$ are uncorrelated. Moreover, since $\boldsymbol{\varepsilon}$ and $\hat{\mathbf{h}}$ are both Gaussian, the channel vector $\mathbf{h}$ can be written as the sum of two statistically independent terms

$$\mathbf{h} = \hat{\mathbf{h}} + \boldsymbol{\varepsilon}. \tag{9}$$

It follows from (8) and (6b) that the components of $\hat{\mathbf{h}}$ are ZM CSCG RVs, the covariance matrix of which is given by

$$\boldsymbol{\mathcal{R}}_{\hat{\mathbf{h}}} \triangleq \mathbb{E}\left[\hat{\mathbf{h}}\hat{\mathbf{h}}^H\right] = \frac{K_{\mathrm{p}}E_{\mathrm{p}}}{N_0}\boldsymbol{\mathcal{R}}\left(\mathbf{I}_L + \frac{K_{\mathrm{p}}E_{\mathrm{p}}}{N_0}\boldsymbol{\mathcal{R}}\right)^{-1}\boldsymbol{\mathcal{R}}. \tag{10}$$

Likewise, the components of $\boldsymbol{\varepsilon}$ are ZM CSCG RVs, the covariance matrix of which is given by

$$\boldsymbol{\mathcal{R}}_{\boldsymbol{\varepsilon}} \triangleq \mathbb{E}[\boldsymbol{\varepsilon}\boldsymbol{\varepsilon}^H] = \left(\mathbf{I}_L + \frac{K_{\mathrm{p}}E_{\mathrm{p}}}{N_0}\boldsymbol{\mathcal{R}}\right)^{-1}\boldsymbol{\mathcal{R}}. \tag{11}$$

For high SNR, i.e., $[K_{\mathrm{p}}E_{\mathrm{p}}/N_0]\boldsymbol{\mathcal{R}}_{i,i} >> 1$ for $1 \leq i \leq L$, the covariance matrix $\boldsymbol{\mathcal{R}}_{\hat{\mathbf{h}}}$ reduces to $\boldsymbol{\mathcal{R}}$ and the elements of the channel noise vector $\boldsymbol{\varepsilon}$ can be considered as i.i.d. ZM CSCG RVs with variance $N_0/(K_{\mathrm{p}}E_{\mathrm{p}})$, since $\boldsymbol{\mathcal{R}}_{\boldsymbol{\varepsilon}}$ becomes

$$\boldsymbol{\mathcal{R}}_{\boldsymbol{\varepsilon}} \approx \frac{N_0}{K_{\mathrm{p}}E_{\mathrm{p}}}\mathbf{I}_L. \tag{12}$$

It follows from (12) that adding more pilot symbols results in a more accurate channel estimate. However, it is important to note that pilot symbols allocate part of the available energy resources. To guarantee a fair comparison of pilot-based receivers in terms of energy use, we introduce E_{b} as the average energy required to transmit one information bit. With $\gamma \triangleq E_{\mathrm{p}}/E_{\mathrm{s}}$ denoting the ratio of E_{p} to E_{s}, it can be shown that the relation between E_{s} and E_{b} is given by

$$E_{\mathrm{s}} = \frac{K}{K + \gamma K_{\mathrm{p}}}\rho\log_2(M)E_{\mathrm{b}}, \tag{13}$$

where M and $\rho \triangleq N_{\mathrm{s}}/(L_{\mathrm{t}}K_{\mathrm{c}})$ denote the constellation size and the code rate, respectively. Hence, for a given energy per information bit E_{b}, the symbol energy E_{s} available for data transmission decreases when more pilot symbols are added.

IV. Mismatched ML receiver

We consider a mismatched maximum likelihood (ML) receiver that uses the estimated channel instead of the true channel. In this way, the ML detection rule of the matrix $\mathbf{B}$ in (6a) is given by

$$\hat{\mathbf{B}} = \arg\min_{\widetilde{\mathbf{B}}}\left\|\mathbf{r} - \sqrt{E_{\mathrm{s}}}\widetilde{\mathbf{B}}\hat{\mathbf{h}}\right\|^2, \tag{14}$$

where the minimization is over all valid code matrices $\widetilde{\mathbf{B}}$. Taking (2) into account, it is readily verified that the detection algorithm (14) reduces to symbol-by-symbol detection for the different information symbols s_i comprised in the matrix $\mathbf{B}$

$$\hat{s}_i = \arg\min_{\tilde{s}}|u_i - \tilde{s}|, \qquad 1 \leq i \leq N_{\mathrm{s}}, \tag{15}$$

where the minimization is over all symbols $\tilde{s}$ belonging to the considered symbol constellation and the decision variable $u_i = u_{i,\mathrm{R}} + ju_{i,\mathrm{I}}$, with $u_{i,\mathrm{R}}$ and $u_{i,\mathrm{I}}$ denoting the real and imaginary parts of u_i, respectively, is given by

$$u_i = \frac{\hat{\mathbf{h}}^H\left(\mathbf{C}_i^* \otimes \mathbf{I}_{L_{\mathrm{r}}}\right)\mathbf{r} + \mathbf{r}^H\left(\mathbf{C}_i^{'T} \otimes \mathbf{I}_{L_{\mathrm{r}}}\right)\hat{\mathbf{h}}}{\lambda\sqrt{E_{\mathrm{s}}}\|\hat{\mathbf{h}}\|^2}. \tag{16}$$

V. Bit error rate analysis

In this section, we derive a closed-form BER expression for OSTBCs under arbitrarily correlated Rayleigh fading with LMMSE channel estimation. Let us consider a rectangular $M_{\mathrm{R}} \times M_{\mathrm{I}}$ QAM constellation Ψ, where the real and imaginary parts of the constellation points are assumed to take M_{R} and M_{I} values out of the sets

$$\Psi'_{\mathrm{R}} = \Big\{(2i-1-M_{\mathrm{R}})d_{\mathrm{R}} \;:\; i=1,2,\ldots,M_{\mathrm{R}}\Big\}, \qquad (17)$$

and

$$\Psi'_{\mathrm{I}} = \Big\{(2i-1-M_{\mathrm{I}})d_{\mathrm{I}} \;:\; i=1,2,\ldots,M_{\mathrm{I}}\Big\}, \qquad (18)$$

respectively. The number M of constellation points in Ψ is given by $M = M_{\mathrm{R}}M_{\mathrm{I}}$. Denoting by b_{R} and b_{I} the real and imaginary parts of a QAM symbol b, respectively, the projections on the real and imaginary axes of the decision area of the symbol b are referred to as the decision regions of b_{R} and b_{I}, respectively. Defining the parameter ξ as $\xi \triangleq d_I^2/d_R^2$ and taking (7) into account, it can be shown that d_{R} and d_{I} are given by

$$d_R = \sqrt{\frac{3}{(M_R^2-1)+(M_I^2-1)\xi}}, \qquad (19)$$

$$d_I = \sqrt{\xi}\, d_R. \qquad (20)$$

In case of square M-QAM, $M_{\mathrm{R}} = M_{\mathrm{I}} = \sqrt{M}$ and $\xi = 1$.

Using the particular channel decomposition (9), the received signal (6a) can be written as

$$\mathbf{r} = \sqrt{E_{\mathrm{s}}}\,\mathbf{B}\hat{\mathbf{h}} + \sqrt{E_{\mathrm{s}}}\,\mathbf{B}\boldsymbol{\varepsilon} + \mathbf{w}, \qquad (21)$$

where $\sqrt{E_{\mathrm{s}}}\,\mathbf{B}\hat{\mathbf{h}}$ is the useful component, $\mathbf{w}$ denotes the Gaussian channel noise, and $\sqrt{E_{\mathrm{s}}}\,\mathbf{B}\boldsymbol{\varepsilon}$ can be treated as an additional noise term caused by the channel estimation error; note that $\hat{\mathbf{h}}$ and $\boldsymbol{\varepsilon}$ are statistically independent. Since the error vector $\boldsymbol{\varepsilon}$ consists of ZM CSCG RVs with covariance matrix (11), the additional noise vector $\sqrt{E_{\mathrm{s}}}\,\mathbf{B}\boldsymbol{\varepsilon}$ is Gaussian when conditioned on the data symbol vector $\mathbf{s}$. Using (21), the decision variable (16) reduces to

$$u_i = s_i + n_i, \qquad 1 \le i \le N_{\mathrm{s}}, \qquad (22)$$

where the disturbance term n_i contains contributions from the channel noise $\mathbf{w}$ and the channel estimation error $\boldsymbol{\varepsilon}$. It is readily verified that $n_i = e_i + w_i$, with

$$e_i = \frac{\hat{\mathbf{h}}^H\left(\mathbf{C}_i^*\mathbf{C}^T \otimes \mathbf{I}_{L_{\mathrm{r}}}\right)\boldsymbol{\varepsilon} + \boldsymbol{\varepsilon}^H\left(\mathbf{C}^*\mathbf{C}_i'^{\,T} \otimes \mathbf{I}_{L_{\mathrm{r}}}\right)\hat{\mathbf{h}}}{\lambda\|\hat{\mathbf{h}}\|^2} \qquad (23)$$

$$w_i = \frac{\hat{\mathbf{h}}^H\left(\mathbf{C}_i^* \otimes \mathbf{I}_{L_{\mathrm{r}}}\right)\mathbf{w} + \mathbf{w}^H\left(\mathbf{C}_i'^{\,T} \otimes \mathbf{I}_{L_{\mathrm{r}}}\right)\hat{\mathbf{h}}}{\lambda\sqrt{E_{\mathrm{s}}}\|\hat{\mathbf{h}}\|^2} \qquad (24)$$

Note that n_i is Gaussian when conditioned on $\mathbf{s}$ and $\hat{\mathbf{h}}$. In case of PCSI, the channel estimation error $\boldsymbol{\varepsilon} = \mathbf{0}$ and n_i is a ZM CSCG RV independent of $\mathbf{s}$ with variance $N_0/(\lambda E_{\mathrm{s}}\|\mathbf{h}\|^2)$. In order to obtain the variance of the disturbance term n_i in case of LMMSE channel estimation, we introduce the $L_{\mathrm{t}} \times L_{\mathrm{t}}$ matrices $\mathbf{C}_{i,\mathrm{R}}(\mathbf{s})$ and $\mathbf{C}_{i,\mathrm{I}}(\mathbf{s})$ as

$$\mathbf{C}_{i,\mathrm{R}}(\mathbf{s}) \triangleq \mathbf{C}\left(\mathbf{C}_i + \mathbf{C}_i'\right)^H, \qquad (25a)$$

$$\mathbf{C}_{i,\mathrm{I}}(\mathbf{s}) \triangleq \mathbf{C}\left(\mathbf{C}_i - \mathbf{C}_i'\right)^H, \qquad (25b)$$

which depend on the data symbol vector $\mathbf{s}$ through the code matrix $\mathbf{C}$. It is readily verified that, when conditioned on $\hat{\mathbf{h}}$ and $\mathbf{s}$, n_i is a ZM non-circularly symmetric complex Gaussian RV, the variances of the real and imaginary parts we denote by $\sigma_{i,\mathrm{R}}^2(\hat{\mathbf{h}},\mathbf{s})$ and $\sigma_{i,\mathrm{I}}^2(\hat{\mathbf{h}},\mathbf{s})$, respectively. With $\mathrm{q} = \mathrm{R}$ or $\mathrm{q} = \mathrm{I}$, it follows from (23)-(25) that $\sigma_{i,\mathrm{q}}^2(\hat{\mathbf{h}},\mathbf{s})$ is given by

$$\sigma_{i,\mathrm{q}}^2(\hat{\mathbf{h}},\mathbf{s}) = \frac{N_0}{2\lambda E_{\mathrm{s}}\|\hat{\mathbf{h}}\|^2}\left(1 + \frac{x_{i,\mathrm{q}}(\hat{\mathbf{h}},\mathbf{s})E_{\mathrm{s}}}{\lambda N_0\|\hat{\mathbf{h}}\|^2}\right), \qquad (26)$$

where $x_{i,\mathrm{q}}(\hat{\mathbf{h}},\mathbf{s})$ is defined as

$$x_{i,\mathrm{q}}(\hat{\mathbf{h}},\mathbf{s}) \triangleq \hat{\mathbf{h}}^H\left(\mathbf{C}_{i,\mathrm{q}}^T(\mathbf{s}) \otimes \mathbf{I}_{L_{\mathrm{r}}}\right)\boldsymbol{\mathcal{R}}_{\boldsymbol{\varepsilon}}\left(\mathbf{C}_{i,\mathrm{q}}^*(\mathbf{s}) \otimes \mathbf{I}_{L_{\mathrm{r}}}\right)\hat{\mathbf{h}}, \qquad (27)$$

and the covariance matrix $\boldsymbol{\mathcal{R}}_{\boldsymbol{\varepsilon}}$ of the channel estimation error $\boldsymbol{\varepsilon}$ is given by (11).

It follows from (26) and (27) that, in general, the variances of the real and imaginary parts of the decision variables (22) are not identical and depend on the index i. Therefore, the BERs corresponding to the in-phase and quadrature bits of the symbols s_i are not necessarily identical and we obtain the BER as

$$P_{\mathrm{b}} = \frac{1}{N_{\mathrm{s}}\log_2(M)}\sum_{i=1}^{N_{\mathrm{s}}}\left[\log_2(M_R)P_{\mathrm{b},i,\mathrm{R}} + \log_2(M_I)P_{\mathrm{b},i,\mathrm{I}}\right], \qquad (28)$$

where $P_{\mathrm{b},i,\mathrm{R}}$ and $P_{\mathrm{b},i,\mathrm{I}}$ denote the BERs of the in-phase and quadrature bits corresponding to the information symbols s_i, respectively. Moreover, since (26) is obtained for given $\hat{\mathbf{h}}$ and $\mathbf{s}$, the BERs of the in-phase and quadrature bits corresponding to s_i can easily be calculated as the average of the corresponding conditional BERs, conditioned on $\hat{\mathbf{h}}$ and $\mathbf{s}$

$$P_{\mathrm{b},i,\mathrm{q}} = \frac{1}{M^{N_{\mathrm{s}}}}\sum_{\mathbf{s}\in\Psi^{N_{\mathrm{s}}}}\mathbb{E}_{\hat{\mathbf{h}}}[P_{\mathrm{b},i,\mathrm{q}}(\hat{\mathbf{h}},\mathbf{s})], \qquad (29)$$

where $\mathrm{q} = \mathrm{R}$ or $\mathrm{q} = \mathrm{I}$, and the conditional BER $P_{\mathrm{b},i,\mathrm{q}}(\hat{\mathbf{h}},\mathbf{s})$ is given by

$$P_{\mathrm{b},i,\mathrm{q}}(\hat{\mathbf{h}},\mathbf{s}) = \frac{1}{\log_2(M_{\mathrm{q}})}\sum_{b_{\mathrm{q}}\in\Psi'_{\mathrm{q}}} d_{\mathrm{H}}(s_{i,\mathrm{q}},b_{\mathrm{q}})\Pr[\hat{s}_{i,\mathrm{q}} = b_{\mathrm{q}}|\hat{\mathbf{h}},\mathbf{s}], \qquad (30)$$

where $d_{\mathrm{H}}(s_{i,\mathrm{q}},b_{\mathrm{q}})$ denotes the Hamming distance between the bits associated to $s_{i,\mathrm{q}}$ and b_{q}, respectively, and $\Pr[\hat{s}_{i,\mathrm{q}} = b_{\mathrm{q}}|\hat{\mathbf{h}},\mathbf{s}]$ is the probability that $u_{i,\mathrm{q}}$ is located inside the decision area of b_{q}, given the channel estimate $\hat{\mathbf{h}}$ and the transmitted symbol vector $\mathbf{s}$. It is readily verified that $\Pr[\hat{s}_{i,\mathrm{q}} = b_{\mathrm{q}}|\hat{\mathbf{h}},\mathbf{s}]$ is given by

$$\Pr[\hat{s}_{i,\mathrm{q}} = b_{\mathrm{q}}|\hat{\mathbf{h}},\mathbf{s}] = Q\left(\sqrt{\frac{D_1^2(s_{i,\mathrm{q}},b_{\mathrm{q}})}{\sigma_{i,\mathrm{q}}^2(\hat{\mathbf{h}},\mathbf{s})}}\right) - Q\left(\sqrt{\frac{D_2^2(s_{i,\mathrm{q}},b_{\mathrm{q}})}{\sigma_{i,\mathrm{q}}^2(\hat{\mathbf{h}},\mathbf{s})}}\right) \qquad (31)$$

where $Q(.)$ is the Gaussian Q-function [12, Eq. (4.1)], and $D_1(s_{i,\mathrm{q}},b_{\mathrm{q}})$ and $D_2(s_{i,\mathrm{q}},b_{\mathrm{q}})$ denote the distances between $s_{i,\mathrm{q}}$ and the boundaries of the decision area of b_{q}, with $D_1(s_{i,\mathrm{q}},b_{\mathrm{q}}) < D_2(s_{i,\mathrm{q}},b_{\mathrm{q}})$; if b_{q} is an outer constellation point, we have $D_2(s_{i,\mathrm{q}},b_{\mathrm{q}}) \to \infty$.

Note that the expectation in (29) requires averaging the Q-functions in (31) over $\hat{\mathbf{h}}$. As (26) is a complicated function of the channel estimate $\hat{\mathbf{h}}$ because of (27), the latter averaging can be performed only numerically. For i.i.d. Rayleigh fading and square OSTBCs, however, it is shown in [7] that (27) reduces to

$$x_{i,\mathrm{q}}(\hat{\mathbf{h}},\mathbf{s}) = \frac{\lambda^2\|\mathbf{s}\|^2}{1+\frac{K_\mathrm{p}E_\mathrm{p}}{N_0}}\|\hat{\mathbf{h}}\|^2, \tag{32}$$

which is irrespective of i and q. More importantly, since the right-hand size of (32) is proportional to $\|\hat{\mathbf{h}}\|^2$, the dependency of the second factor in (26) on $\hat{\mathbf{h}}$ disappears and (26) becomes a function of $\hat{\mathbf{h}}$ through an inverse proportionality to $\|\hat{\mathbf{h}}\|^2$ only. Considering that for i.i.d. Rayleigh fading, the squared norm $\|\hat{\mathbf{h}}\|^2$ follows a χ^2-distribution, this permits to derive a closed-form BER expression, as shown in [7]. If the channel coefficients are not i.i.d. or if the OSTBC matrix is not square, however, (26) is clearly not inversely proportional to $\|\hat{\mathbf{h}}\|^2$, and an exact closed-form BER expression cannot be found. Nevertheless, in order to obtain a closed-form BER expression for these cases as well, (32) inspires us to approximate $x_{i,\mathrm{q}}(\hat{\mathbf{h}},\mathbf{s})$ as follows

$$x_{i,\mathrm{q}}(\hat{\mathbf{h}},\mathbf{s}) \approx \alpha_{i,\mathrm{q}}(\mathbf{s})\,\|\hat{\mathbf{h}}\|^2, \tag{33}$$

where we use a minimum mean-square error (MMSE) criterion to obtain the proportionality factor $\alpha_{i,\mathrm{q}}(\mathbf{s})$

$$\alpha_{i,\mathrm{q}}(\mathbf{s}) = \arg\min_{\tilde{\alpha}} \mathbb{E}\left[\left|x_{i,\mathrm{q}}(\hat{\mathbf{h}},\mathbf{s}) - \tilde{\alpha}\,\|\hat{\mathbf{h}}\|^2\right|^2\right]. \tag{34}$$

It can be shown that (34) yields

$$\alpha_{i,\mathrm{q}}(\mathbf{s}) = \frac{\mathrm{tr}(\boldsymbol{\mathcal{R}}_{\hat{\mathbf{h}}})\mathrm{tr}\left(\mathbf{A}_{i,\mathrm{q}}(\mathbf{s})\boldsymbol{\mathcal{R}}_{\hat{\mathbf{h}}}\right) + \mathrm{tr}\left(\boldsymbol{\mathcal{R}}_{\hat{\mathbf{h}}}\mathbf{A}_{i,\mathrm{q}}(\mathbf{s})\boldsymbol{\mathcal{R}}_{\hat{\mathbf{h}}}\right)}{\mathrm{tr}(\boldsymbol{\mathcal{R}}_{\hat{\mathbf{h}}})\mathrm{tr}(\boldsymbol{\mathcal{R}}_{\hat{\mathbf{h}}}) + \mathrm{tr}(\boldsymbol{\mathcal{R}}_{\hat{\mathbf{h}}}\boldsymbol{\mathcal{R}}_{\hat{\mathbf{h}}})}, \tag{35}$$

where $\mathbf{A}_{i,\mathrm{q}}(\mathbf{s})$ is defined as

$$\mathbf{A}_{i,\mathrm{q}}(\mathbf{s}) \triangleq \left(\mathbf{C}_{i,\mathrm{q}}^T(\mathbf{s})\otimes\mathbf{I}_{L_\mathrm{r}}\right)\boldsymbol{\mathcal{R}}_{\boldsymbol{\varepsilon}}\left(\mathbf{C}_{i,\mathrm{q}}^*(\mathbf{s})\otimes\mathbf{I}_{L_\mathrm{r}}\right). \tag{36}$$

Using the approximation (33), the variance (26) of the real and imaginary parts of n_i reduces to

$$\sigma_{i,\mathrm{q}}^2(\hat{\mathbf{h}},\mathbf{s}) = \frac{N_0}{2\lambda E_\mathrm{s}\|\hat{\mathbf{h}}\|^2}\left(1+\frac{\alpha_{i,\mathrm{q}}(\mathbf{s})E_\mathrm{s}}{\lambda N_0}\right), \tag{37}$$

and a closed-form BER expression for arbitrarily correlated Rayleigh fading can be obtained in a similar way as in [7], since the probability density function (PDF) of $\|\hat{\mathbf{h}}\|^2$ is shown to reduce to a weighted sum of χ^2-distributions [13]

$$p_{\|\hat{\mathbf{h}}\|^2}(x) = \sum_{m=1}^{\kappa}\sum_{n=1}^{c_m}\frac{D_{m,n}}{(n-1)!\,(\lambda_m)^n}\,x^{n-1}\,\exp\left(-\frac{x}{\lambda_m}\right), \tag{38}$$

where $x \geq 0$, and λ_m denotes the m-th distinct eigenvalue of $\boldsymbol{\mathcal{R}}_{\hat{\mathbf{h}}}$ with corresponding algebraic multiplicity c_m. In (38), the parameter $D_{m,n}$ is given by

$$D_{m,n} = \frac{(\lambda_m)^{n-c_m}}{(c_m-n)!}\left[\frac{\mathrm{d}^{c_m-n}}{\mathrm{d}s^{c_m-n}}F(s)\,(1+\lambda_m\,s)^{c_m}\right]\Big|_{s=-\frac{1}{\lambda_m}}, \tag{39}$$

where

$$F(s) = \prod_{l=1}^{\kappa}(1+\lambda_l\,s)^{-c_l}. \tag{40}$$

Using the approximation (33), it follows from (37) and [14, 14.4-15] that averaging the Q-functions in (31) over $\|\hat{\mathbf{h}}\|^2$ results in the following closed-form expression

$$\mathbb{E}_{\hat{\mathbf{h}}}\left[Q\left(\sqrt{\frac{D_\nu^2(s_{i,\mathrm{q}},b_\mathrm{q})}{\sigma_{i,\mathrm{q}}^2(\hat{\mathbf{h}},\mathbf{s})}}\right)\right] = \sum_{m=1}^{\kappa}\sum_{n=1}^{c_m}D_{m,n} \times\left[\frac{1-\mu_m}{2}\right]^n\sum_{k=0}^{n-1}\binom{n-1+k}{k}\left[\frac{1+\mu_m}{2}\right]^k, \tag{41}$$

where $\nu = \{1,2\}$, and μ_m is given by

$$\mu_m \triangleq \left[\frac{\lambda D_\nu^2(s_{i,\mathrm{q}},b_\mathrm{q})\frac{E_\mathrm{s}}{N_0}\left(1+\frac{\alpha_{i,\mathrm{q}}(\mathbf{s})}{\lambda}\frac{E_\mathrm{s}}{N_0}\right)^{-1}\lambda_m}{1+\lambda D_\nu^2(s_{i,\mathrm{q}},b_\mathrm{q})\frac{E_\mathrm{s}}{N_0}\left(1+\frac{\alpha_{i,\mathrm{q}}(\mathbf{s})}{\lambda}\frac{E_\mathrm{s}}{N_0}\right)^{-1}\lambda_m}\right]^{\frac{1}{2}}. \tag{42}$$

From (41)-(42) and (28)-(31), a closed-form BER expression for OSTBCs employing rectangular QAM on arbitrarily correlated Rayleigh fading channels with pilot-based LMMSE channel estimation, is readily obtained.

In case of i.i.d. Rayleigh fading and square QAM constellations, the resulting BER expression can be easily shown to reduce to the exact BER result for square OSTBCs and to the approximate BER result for non-square OSTBCs in [7]. Furthermore, by applying the high-SNR approximation (12) to (36), the presented BER expression converges to the asymptotically exact BER result from [8] for square OSTBCs and square QAM constellations on arbitrarily correlated Rayleigh fading channels. However, as the above derivation does not rely on any high-SNR approximation, the resulting BER expression yields more accurate results for low-to-moderate SNR than the asymptotic expression from [8]. Moreover, it also allows to obtain very accurate BER results for non-square OSTBCs as well as rectangular QAM constellations.

VI. Numerical results

Using Monte-Carlo simulations, we illustrate the accuracy of the presented closed-form BER approximation under the assumption that $E_\mathrm{p} = E_\mathrm{s}$ and $\xi = 1$.

Fig. 1 displays the BER for the 3×4 OSTBC given by [2]

$$\mathbf{C} = \frac{2}{\sqrt{3}}\begin{bmatrix} s_1 & -s_2^* & \frac{s_3^*}{\sqrt{2}} & \frac{s_3^*}{\sqrt{2}} \\ s_2 & s_1^* & \frac{s_3^*}{\sqrt{2}} & -\frac{s_3^*}{\sqrt{2}} \\ \frac{s_3}{\sqrt{2}} & \frac{s_3}{\sqrt{2}} & \frac{-s_1-s_1^*+s_2-s_2^*}{2} & \frac{s_2+s_2^*+s_1-s_1^*}{2}\end{bmatrix}, \tag{43}$$

where the scaling factor $2/\sqrt{3}$ is applied in order that (43) satisfies (2). Assuming a dual-antenna receiver ($L_\mathrm{r} = 2$), we show the BER curves for rectangular $M_\mathrm{R}\times M_\mathrm{I}$ QAM constellations. The covariance matrix $\boldsymbol{\mathcal{R}}$ of the correlated Rayleigh fading channels is assumed to be given by $\boldsymbol{\mathcal{R}} = \boldsymbol{\mathcal{R}}_\mathrm{t}\otimes\boldsymbol{\mathcal{R}}_\mathrm{r}$, where the transmit covariance matrix $\boldsymbol{\mathcal{R}}_\mathrm{t}$ and the receive covariance matrix $\boldsymbol{\mathcal{R}}_\mathrm{r}$ are given by

$$\boldsymbol{\mathcal{R}}_\mathrm{t} = \begin{bmatrix} 1 & 0.7+j0.3 & 0.4-j0.2 \\ 0.7-j0.3 & 1 & 0.5+j0.1 \\ 0.4+j0.2 & 0.5-j0.1 & 1\end{bmatrix}, \tag{44a}$$

$$\boldsymbol{\mathcal{R}}_\mathrm{r} = \begin{bmatrix} 1 & 0.8 \\ 0.8 & 1\end{bmatrix}. \tag{44b}$$

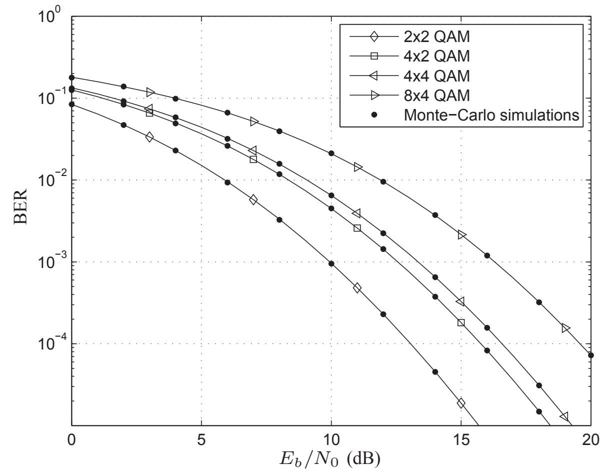

Fig. 1. BER for the 3×4 OSTBC given by (43) with rectangular $M_{\mathrm{R}} \times M_{\mathrm{I}}$ QAM transmission on correlated Rayleigh fading channels.

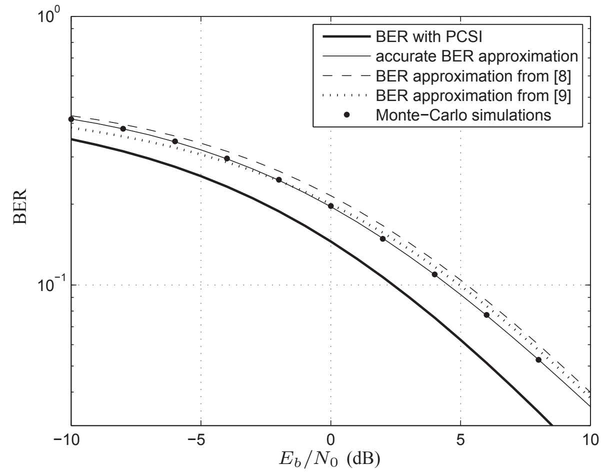

Fig. 2. BER for Alamouti's code. Both the curves from the presented accurate closed-form BER approximation and from the high-SNR approximations in [8] and [9] are shown.

Furthermore, we assume pilot-based LMMSE channel estimation with $K = 100$ and $K_{\mathrm{p}} = 16$. Monte-Carlo simulations indicate that the presented BER approximation yields very accurate results in the range from low to high SNR.

In Fig. 2, we show that the presented closed-form BER expression yields significantly more accurate results than the high-SNR BER approximations from [8] and [9], in particular in the case of low-to-medium SNR. Since the asymptotically exact BER approximation from [8] is defined for square OSTBCs only, we consider the square 2×2 Alamouti code, which is given by [1]

$$\mathbf{C} = \left[\begin{array}{cc} s_1 & -s_2^* \\ s_2 & s_1^* \end{array} \right]. \tag{45}$$

Assuming a single-antenna receiver ($L_{\mathrm{r}} = 1$), the covariance matrix $\boldsymbol{\mathcal{R}}$ describing the correlation between the highly correlated Rayleigh fading channel coefficients is given by

$$\boldsymbol{\mathcal{R}} = \left[\begin{array}{cc} 1 & 0.99 \\ 0.99 & 1 \end{array} \right]. \tag{46}$$

Furthermore, we consider 4-QAM transmission and LMMSE channel estimation with $K = 20$ and $K_{\mathrm{p}} = 4$. In Fig. 2, Monte-Carlo simulations indicate that, even in the case of low-to-medium SNR and highly correlated channels, the generalized closed-form BER approximation presented in this contribution remains very accurate, in contrast with the BER approximations from [8] and [9]. This is due to the fact that no high-SNR approximation is used in the analysis in section V.

VII. Conclusions

In this contribution, we examined the BER performance of OSTBCs under arbitrarily correlated Rayleigh fading channels with LMMSE channel estimation. We presented a generalized closed-form BER approximation for rectangular QAM constellations, which yields very accurate BER results from low to high SNR.

References

[1] S. M. Alamouti, "A simple transmit diversity technique for wireless communications," *IEEE J. Select. Areas Commun.*, vol. 16, pp. 1459–1478, Oct. 1998.

[2] V. Tarokh, H. Jafarkhani, and A. R. Calderbank, "Space-time block codes from orthogonal designs," *IEEE Trans. Inform. Theory*, vol. 45, no. 5, pp. 1456–1467, Jul. 1999.

[3] A. Maaref and S. Aissa, "On the error probability performance of transmit diversity under correlated Rayleigh fading," in *IEEE Radio and Wireless Conference*, Sep. 2004, pp. 275–278.

[4] I.-M. Kim, "Exact BER analysis of OSTBCs in spatially correlated MIMO channels," *IEEE Trans. Commun.*, vol. 54, no. 8, pp. 1365–1373, Aug. 2006.

[5] A. Maaref and S. Aissa, "Performance analysis of orthogonal space-time block codes in spatially correlated MIMO Nakagami fading channels," *IEEE Trans. Wireless Commun.*, vol. 5, no. 4, pp. 807–817, Apr. 2006.

[6] ——, "Exact error probability analysis of rectangular QAM for single- and multichannel reception in Nakagami-m fading channels," *IEEE Trans. Commun.*, vol. 57, no. 1, pp. 214–221, Jan. 2009.

[7] L. Jacobs and M. Moeneclaey, "Effect of MMSE channel estimation on BER performance of orthogonal space-time block codes in Rayleigh fading channels," *IEEE Trans. Commun.*, vol. 57, no. 5, pp. 1242–1245, May 2009.

[8] ——, "BER analysis of square OSTBCs with LMMSE channel estimation in arbitrarily correlated Rayleigh fading channels," *IEEE Commun. Lett.*, vol. 14, no. 7, pp. 626–628, Jul. 2010.

[9] L. Jacobs, G. Alexandropoulos, M. Moeneclaey, H. Bruneel, and P. Mathiopoulos, "Analysis and efficient evaluation of the BER of OSTBCs with imperfect channel estimation in arbitrarily correlated fading channels," *IEEE Trans. Signal Process.*, vol. 59, no. 6, pp. 2720–2733, Jun. 2011.

[10] X.-B. Liang, "Orthogonal designs with maximal rates," *IEEE Trans. Inform. Theory*, vol. 49, no. 10, pp. 2468–2503, Oct. 2003.

[11] G. Taricco, "Optimum receiver design and performance analysis of arbitrarily correlated Rician fading MIMO channels with imperfect channel state information," *IEEE Trans. Inform. Theory*, vol. 56, no. 3, pp. 1114–1134, Mar. 2010.

[12] M. K. Simon and M.-S. Alouini, *Digital Communication over Fading Channels*, New York: Wiley, 2nd ed., 2005.

[13] C. Siriteanu and S. Blostein, "Performance and complexity analysis of eigencombining, statistical beamforming, and maximal-ratio combining," *IEEE Trans. Veh. Technol.*, vol. 58, no. 7, pp. 3383–3395, Sep. 2009.

[14] J. Proakis, *Digital Communications*, McGraw-Hill, 4th ed., 2001.